BUILDING ROOF CONTOUR EXTRACTION FROM LiDAR DATA

Aluir P. Dal Poz, Professor
Dept. of Cartography
College of Sciences and Technology
São Paulo State University
R. Roberto Simonsen 305
19060-900 Presidente Prudente, SP, Brazil
aluir@fct.unesp.br

Edinéia A. S. Galvanin, Associate Professor
Dept. of Mathematics
Mato Grosso State University
R. A, s/n, 78390-000, Barra do Bugres, MT, Brazil
galvanin@gmail.com

ABSTRACT

This paper proposes a method for the automatic extraction of building roof contours from a LiDAR-derived digital surface model (DSM). The method is based on two steps. First, to detect aboveground objects (buildings, trees, etc.), the DSM is segmented through a recursive splitting technique followed by a region merging process. Vectorization and polygonization are used to obtain polyline representations of the detected aboveground objects. Second, building roof contours are identified from among the aboveground objects by optimizing a Markov-random-field-based energy function that embodies roof contour attributes and spatial constraints. Preliminary results have shown that the proposed methodology works properly.

KEYWORDS: Building Roof Contours, DSM, Markov Random Field, Simulated Annealing

INTRODUCTION

Automated building extraction from LiDAR data or LiDAR-derived data has received increasing attention in recent years. Published methods for building detection or extraction from these data can be grouped into the following categories: building detection, building roof contour extraction, building roof extraction, and building model extraction. Building detection is performed using a digital surface model (DSM) (Matikainen et al., 2003), a normalized DSM (Tóvari and Vögtle, 2004), or a LiDAR point cloud (Tarsha-Kurdi et al., 2006). Typically, methods for building roof contour extraction firstly detect irregular building roof contours and then subjected them to a regularization process, like the method proposed by Sampath and Shan (2007) for extracting building roof contours from a LiDAR point cloud. Building roof extraction is performed using segmentation methods, which group LiDAR point cloud data into planar faces and other objects. Examples of algorithms for segmenting LiDAR point cloud data into roof planar faces can be found in Maas and Vossel (1999) and Rottensteiner et al. (2005). Building model extraction involves building detection, building roof contour extraction, and building roof extraction. Dorninger and Pfeifer (2008) have described an approach for the automated determination of 3D city models from LiDAR point cloud data that takes into account the basic assumption that individual buildings can be properly modeled as a composition of planar faces.

In this paper, a method for building roof contour extraction from a LiDAR-derived DSM is proposed. Our methodology is based on the concept of first extracting aboveground objects and then identifying those objects that are building roof contours. This paper is organized as follows: next section presents the proposed method; then, experimental results are presented and discussed; and the main conclusions and future perspectives are summarized in last section.

METHOD

Our method for building roof contour extraction from a LiDAR derived DSM is based on two steps: 1) automatic extraction of aboveground object polylines from the DSM; and 2) recognition of polylines extracted in step 1 that represent building roof contours.

Extraction of Aboveground Objects

Our algorithm for automatic extraction of aboveground regions starts segmenting the DSM into aboveground and ground objects. First, the DSM is segmented by using the recursive splitting technique (Jain et al., 1995). The second step consists of grouping adjacent regions of similar heights in such a way that over-segmentation that is typical of the recursive splitting technique is minimized and the resulting regions correspond to either ground or aboveground objects. Our basic supposition is that the object of interest (Buildings) is at least 3 m tall. The fundamental result of the segmentation process is a binary grid where ground grid points are assigned a zero value and aboveground grid points are assigned a value of one.

Because our strategy (see next subsection) for identifying building roof contours requires that aboveground regions (buildings and other objects - e.g. trees) be represented by polylines, we applied sequentially a contour following algorithm (Ballard and Brown, 1982) for generating ordered lists of contour points and the Douglas-Peucker algorithm to generate polyline representations for the ordered lists of contour points.

Identification of Building Roof Contour Polylines Using an MRF Model

In an MRF model, the sites S={1, …, n} are related to one another through a neighborhood system defined as $\eta = \{\eta_i, i \in S\}$, where η_i is the set of sites neighboring i. According to the Hammersley-Clifford theorem, an MRF can be characterized by a Gibbs probability distribution (Kopparapu and Desai, 2001), i.e.:

$$P(\mathbf{x}) = \frac{\exp(-U(\mathbf{x}))}{Z} \tag{1}$$

$$Z = \sum_{\mathbf{x} \in \mathbf{X}} \exp(-U(\mathbf{x})) \tag{2}$$

where, $\mathbf{x}$ is a configuration of a random field X, $\mathbf{X}$ is the set of all possible configurations of the random field X, and $U(\mathbf{x})$ is an energy function, which can be expressed as:

$$U(\mathbf{x}) = \sum_{c \in C} V_c(\mathbf{x}) \tag{3}$$

Equation 3 shows that the energy function is a sum of clique potentials ($V_c(\mathbf{x})$) over all possible cliques $c \in C$. A clique c is a subset of sites in S in which every pair of distinct sites are neighbors. The value of $V_c(\mathbf{x})$ depends on the local configuration of clique c.

Polylines representing building roof contours can be found by analyzing the aboveground region polylines. We formulated this problem as an MRF where the energy function takes the following mathematical form:

$$U(\mathbf{x}) = U(p_1, \ldots, p_n) = \alpha \sum_{i=1}^{n} |p_i - r_i| + \beta \sum_{i=1}^{n} \frac{(1-p_i)}{A_i} - \omega \sum_{i=1}^{n} \sum_{j \in \eta_i} p_i p_j \left|\cos(2\theta_{ij})\right| - \gamma \sum_{i=1}^{n} \left[p_i \ln p_i + (1 - p_i) \ln (1 - p_i) \right] \tag{4}$$

In Equation 4, p_i is a parameter that varies over [0; 1] and converges to one if the region R_i is interpreted as a building roof contour; otherwise, p_i converges to zero. In addition, n is the number of regions, and α, β, ω, and γ are positive constants that express the relative importance of the following energy terms: rectangularity energy; area energy; spatial energy; and entropy energy.

The rectangularity energy term favors rectilinear regions and depends on the rectangularity attribute $r_i = |sen\theta_i|$, in which θ_i is the angle between the two main directions of the region R_i. The optimal value of attribute r_i is one, meaning that the region polyline R_i contains only pairs of straight lines that are either parallel or perpendicular to one another. The area energy term favors larger regions and depends on the area A_i of the region R_i. The spatial energy term benefits polyline regions that have main axis directions that are approximately parallel or perpendicular to one another. In this term, θ_{ij} is the angle between the main axis directions of polyline regions R_i and R_j. This energy term also depends on the components (η_i) of the neighborhood system, which is defined as follows:

$$\eta_i = \{R_j \mid dist(R_j, R_i) \leq d\} \quad (5)$$

where, function *dist* is given by the Euclidean distance between the centroids of the two regions R_i and R_j, and d is a distance threshold. The entropy energy term depends on p_j (which can be interpreted as the probability of region R_i being a building roof contour). The purpose of this term is to force p_j to converge to either one or zero.

We used the simulated annealing (SA) algorithm to find the optimal solution (p_1, …, p_n) that minimizes the energy function U. According to Kopparapu and Desai, 2001, SA algorithm is usually effective in finding the global minimum, even when the energy function has local minima.

EXPERIMENTAL RESULTS

The proposed approach is implemented using Borland C++ Builder 5 compiler for Windows XP and the input DSM is generated by the SPRING freeware developed by INPE (National Institute for Space Research), Brazil, which is available at http://www.dpi.inpe.br/spring/english/index.html. The nearest-neighbor interpolation method was used for generating a 70-cm-resolution DSM. The LiDAR data set used here was obtained from Curitiba, Brazil. Constants of the energy function U were empirically determined to be $\alpha = \beta = \gamma = 0.7$ and $\omega = 0.99$.

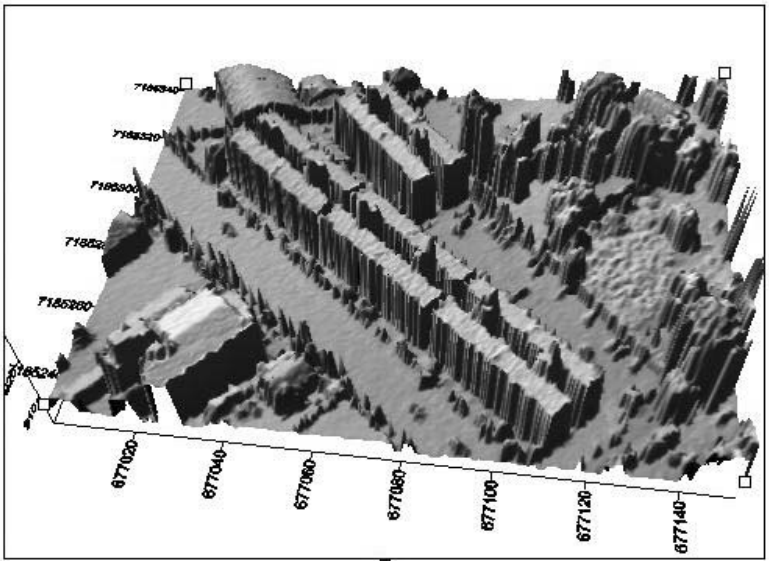

Figure 1. Three-dimensional visualization of the test area DSM.

Below, we present and analyze the preliminary results obtained for one small test area, which is visualized in 3D in Figure 1. Five buildings can be readily identified, with three of them being aligned and almost attached. Figure 2(a) (showing intensity image obtained from the laser pulse return intensity) shows another building, which is not identifiable in Figure 1, near the upper-right corner of the intensity image (see the arrow in black).

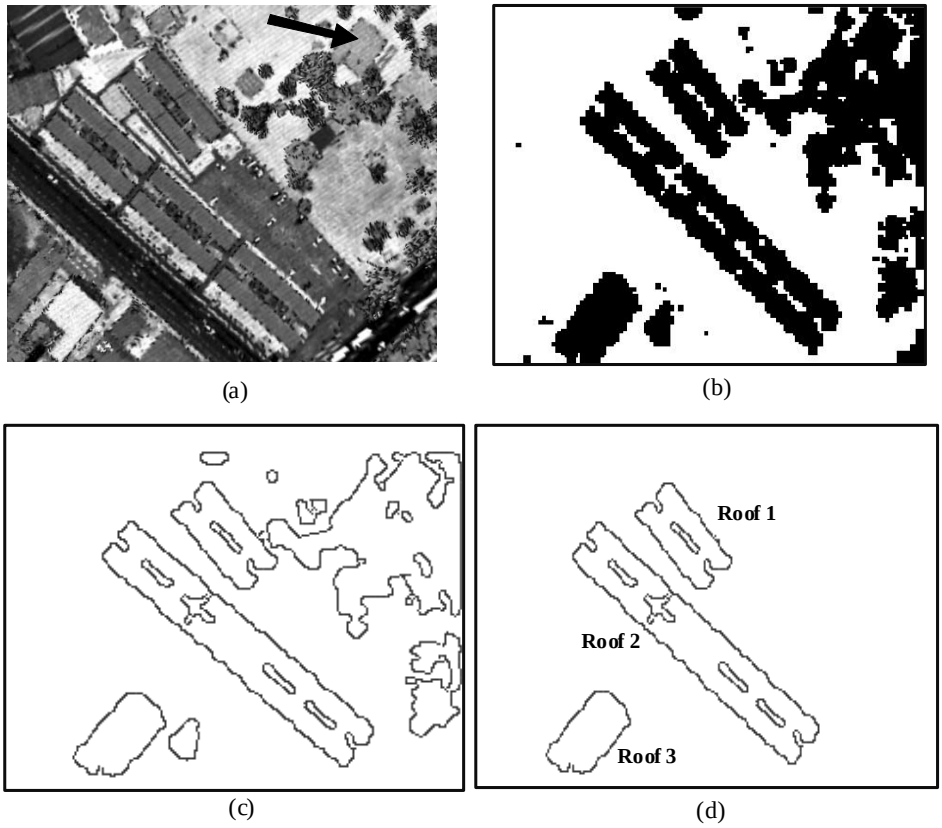

Figure 2. Results obtained. (a) Intensity image showing test area; (b) Aboveground regions; (c) Contours of the aboveground regions; and (d) Identified building roof contours.

The detected aboveground regions (dark areas) present in test area are displayed in Figure 2(b) using a binary grid. The corresponding polylines are visualized in Figure 2(c). Figures 2(b) and 2(c) also show that an aboveground region representing the building surrounded by trees near the upper-right corner of the intensity image (see the arrow in Figure 2(a)) was not detected. Also note this corresponding area in Figure 1. Figure 2(d) shows that the proposed method correctly identified all of the buildings, with the exception of the building that was not detected in the first step of our method. Please note that all extracted buildings had relatively regular shapes and favorable spatial orientation (approximately parallel or perpendicular to one another). These are key characteristics to correctly identifying buildings by minimizing the proposed energy function. Please also note that the three aligned buildings were merged in the first step of our methodology (see Figures 2(b) and 2(c)). As a result, only a single long building is identified in the second step.

CONCLUSIONS AND FUTURE PERSPECTIVES

A method for the automatic extraction of building roof contours from a LiDAR-based DSM was proposed and evaluated in this paper. The method is a two-step process. First, polylines representing contours of aboveground objects are extracted from the DSM. Next, an MRF-based energy function is used to identify polylines that correspond to building roof contours. In order to preliminarily exemplify the performance of the proposed approach, we presented and

analyzed the results obtained for one test area. The method correctly identified all of the buildings, with the exception of the building, indicating that it is promising.

As a perspective for this paper, some improvements in the method can enhance the performance of the proposed method. For example, a pre-processing step for detecting and removing trees could allow the method to identify the building not detected in test area used in our preliminary experiment. Also, in order to provide a realist evaluation of the proposed method, it will be necessary to accomplish several experiments involving varied landscape complexities. Moreover, different DSM accuracies and resolutions are important features to be analyzed in the context of the performance of the method.

ACKNOWLEDGEMENTS

This work was supported by CNPq (National Council for Scientific and Technological Development - Brazil), grant numbers 307116/2006-9 and 304879/2009-6. The LiDAR data used in our experiments was provided by LACTEC, Curitiba, Pr – Brazil.

REFERENCES

Ballard, D. H., and C. M. Brown, 1982. *Computer Vision*, Prentice Hall, Inc., Englewood Cliffs, New Jersey, 523p.

Jain, R., R. Kasturi, and B. G. Schunck, 1995. *Machine vision*, MIT Press and McGraw-Hill, Inc New York, 549.

Kopparapu, S. K., and U. B. Desai, 2001. *Bayesian Approach to Image Interpretation*, 127p.

Matikainen, L., J. Hyyppä, and H. Hyyppä, 2003. Automatic detection of buildings from laser scanner data for map updating, In: *Int. Arch. Photogramm. Remote Sensing*, Dresden-Germany, Vol. 34 Part, 3/W13, Dresden, Germany.

Rottensteiner, F., J. Trinder, S. Clode, and K. Kubik, 2005. Automated delineation of roof planes from LIDAR Data. In: *Int. Arch. Photogramm. Remote Sensing Spatial Information Sciences*, Enschede-The Netherlands, Vol. 36, pp. 221-226.

Sampath, A., and J. Shan, 2007. Building boundary tracing and regularization from airborne Lidar point clouds, *Photogrammetric Engineering and Remote Sensing*, 73(7): 805-812.

Tarsha-Kurdi, F., T. Landes, P. Grussenmeyer, and E. Smigiel, 2006. New Approach for Automatic Detection of Buildings in Airborne Laser Scanner Data Using first Echo only, In: Symposium of ISPRS Comm. III Photogramm. Computer Vision. Bonn-Germany.

Tóvari, D., and T. Vögtle, 2004. Object classification in laserscanning data. In: *International Int. Arch. Photogramm. Remote Sensing Spatial Information Sciences*, Freibur-Germany, Vol. 36, pp. 45–49.